

# DESIGN STUDY FOR THE GENERATION OF FEW-CYCLE FEL PULSES USING MODE-LOCKED AFTERBURNER SCHEME AT CLARA

C. L. Shurvinton, D. J. Dunning, N. R. Thompson  
ASTeC & CI, STFC Daresbury Laboratory, Daresbury, UK

## Abstract

Ultrashort pulse operation in FELs is a highly desirable capability for imaging matter on ultrafast timescales. This paper presents a design study for a proof-of-principle demonstration of the mode-locked afterburner (ML-AB) scheme on the FEL test facility CLARA. A start-to-end simulation has been constructed using the time-dependent three-dimensional FEL code GENESIS 1.3 to evaluate the performance of the scheme. The ability to produce pulses of several femtoseconds in duration with peak powers of the order of 100 MW at 100 nm wavelength is predicted. Such pulses have duration of 2 fs (6 optical cycles), a factor of ~5 shorter than the FEL cooperation length. Potential routes for further optimisation and alternative operating modes are explored.

## CLARA AND ML-AB OVERVIEW

CLARA is a FEL test facility currently under construction at Daresbury laboratory, designed to operate in the UV regime between 100-400nm [1]. It is planned to implement several novel accelerator and FEL schemes on CLARA as part of R&D for a potential upcoming UK XFEL [2]. The mode-locked afterburner (ML-AB) is one such scheme, designed as a potential source of few-cycle photon pulse trains of high power [3].

The scheme has three main sections, as seen in Fig. 1. It operates by inducing an energy modulation in the preliminary “modulator” section, which then creates periodic regions of strong bunching along the main “amplifier” radiator section. These strongly bunched regions are then mapped to a fine short pulse train structure using an additional “afterburner” section consisting of short radiator modules separated by chicanes. Since the requirements of the amplifier section are generic, it is hoped that this afterburner section could be installed on the end of existing FELs to add short-pulse capability to existing facilities. At the current stage of development it is necessary to identify certain key parameters, such as the required seed laser power for the modulator stage, as well as to construct a more robust model to test the feasibility and tolerances of the scheme.

## SIMULATION AND OPTIMISATION

Simulations were performed using the time-dependent 3D FEL code GENESIS 1.3 [4]. The three different sections of the scheme were each modelled separately, and the particle and field distributions then imported into the next section. A short Python script was used to automate the start-to-end process. The parameters used in the simulation are seen in Table 1. These now represent outdated parameters for the

CLARA lattice, but since the requirements of the amplifier section are generic the results presented hold as a proof of concept for the scheme.

Table 1: Parameters Used for Simulation

Parameter	Value
Electron beam energy [MeV]	250
Peak Current [A]	400
$\rho$ parameter	$2.57 \times 10^{-3}$
Normalised emittance [mm-mrad]	0.5
RMS energy spread, $\sigma_\gamma / \gamma_0$	$9.78 \times 10^{-5}$
Undulator period, $\lambda_u$ [mm]	29
Undulator periods per amplifier module	86
Undulator periods per afterburner module	8
Resonant wavelength, $\lambda_r$ [nm]	100
Modulation period, $\lambda_m$ [ $\mu\text{m}$ ]	3
Cooperation Length, $l_c$ [ $\mu\text{m}$ ]	3.10

Previous simulations [1, 3] have already demonstrated the theoretical feasibility and potential output capability of this scheme, but to undergo a more thorough investigation it was necessary to do a parameter scan to determine a new baseline optimal working point and output. After optimising the amplifier and afterburner modules for steady-state performance using GENESIS 1.3, different configurations of the scheme were investigated to find an optimal setup. The parameters considered were the magnitude of energy modulation, which was controlled via the seed laser power in the modulator section, and the numbers of modules used in the amplifier and afterburner sections.

A merit function was defined to identify an optimal working point. The M-function used was

$$M = \ln(P_{pk}) \left( \frac{P_{pk} - P_t}{P_{pk} + P_t} \right), \quad (1)$$

where  $P_{pk}$  is the peak power and  $P_t$  is the trough power, defined as the lowest power on either side of an individual pulse. The effect of changing seed laser power and number of amplifier modules on the merit function of the final output of the scheme, for a 10-module afterburner configuration, is seen in Fig. 2. The merit function shows a clear peak for both the 4- and 6-amplifier-module configurations.

After an optimal amplifier configuration was determined, the power growth through the afterburner was also studied to ensure there were enough modules for exponential growth to reach saturation. This is seen in Fig. 3, which shows that saturation is reached by the 11th module.

Based on these results the configuration chosen as the baseline optimal working point used a 62.5 MW seed laser,

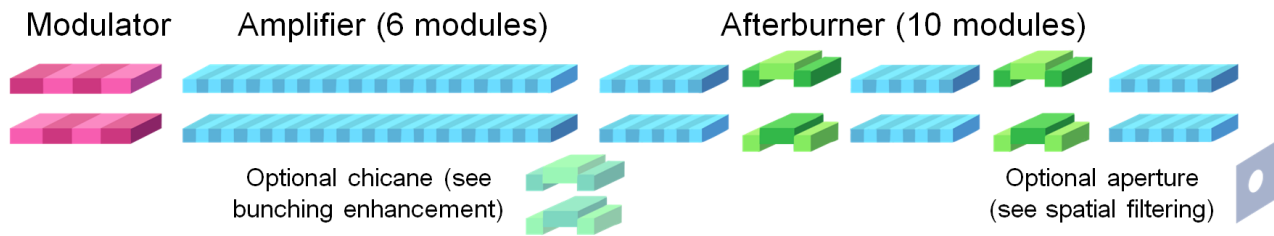


Figure 1: Schematic showing the relevant components and operation of the scheme.

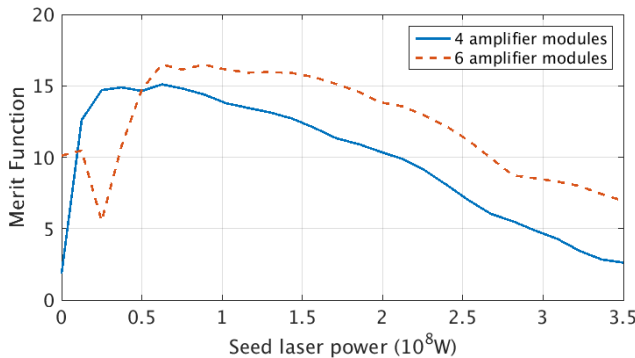


Figure 2: Variance of merit function for different configurations of the baseline scheme.

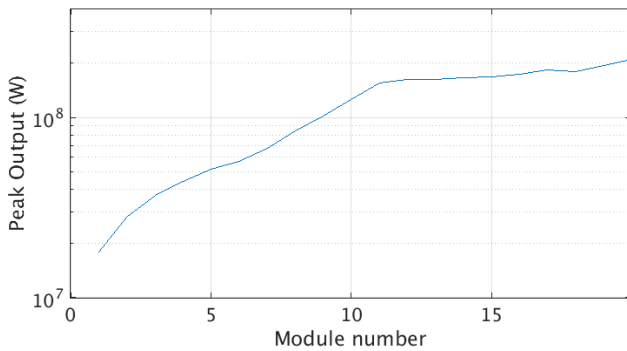


Figure 3: Growth of the peak output power through the afterburner modules.

6 amplifier modules and 10 afterburner modules, as this represented a peak on the merit function and included enough afterburner modules for the pulse to reach saturation. The

Table 2: Scheme Output Comparison

Scheme	Peak Power [W]	Pulse Duration [fs]	M
Baseline	$1.26 \times 10^8$	2.0	16.5
Enhanced Bunching	$2.19 \times 10^8$	2.7	17.5
Aperture Filtering	$1.18 \times 10^8$	2.0	17.5

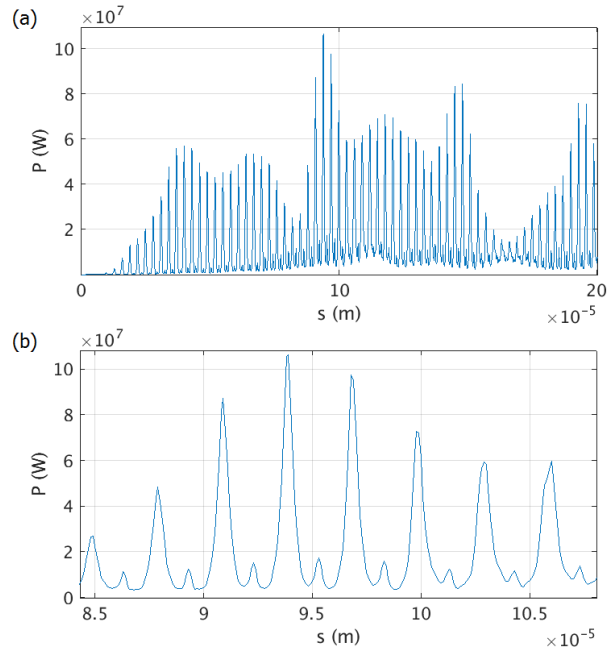


Figure 4: Time domain output for the baseline operating mode, (a) showing the full pulse and (b) a detail shot of the clean pulse train produced.

resulting baseline output can be seen in Fig. 4, and the output parameters are shown in the first row of Table 2.

### ALTERNATIVE OPERATING MODE - BUNCHING ENHANCEMENT

The two main factors influencing the final output of the scheme are the level of bunching and the radiation power generated in the amplifier. A larger energy modulation is needed to enable a strongly defined bunching structure to develop in the amplifier section. This means, however, that the power output grows more slowly and this limits the peak power obtained from the scheme. An alternative mode of operation was proposed which included a chicane in between the amplifier and the afterburner sections to optimise the bunching factor prior to the afterburner section.

To simulate this an  $R_{56}$  transformation was applied to the particle distribution at the beginning of the afterburner. The scheme was tested on several alternative amplifier/seed power configurations to see whether the output could be improved compared to the default case.

It was found that this scheme produces the strongest pulses when applied to configurations with a lower seed power, as the weaker energy modulation causes the radiation power to grow faster in the amplifier section. This also allows for the amplifier section to be shorter, which reduces energy spread and allows for faster growth in the afterburner section. The bunching structure created is comparatively weaker, but the chicane compensates for this.

The pulse obtained from this scheme with the highest peak power is shown in Fig. 5, with the output parameters shown in Table 2. This pulse was generated using a 15 MW seed laser in the modulator, compared to 62.5 MW in the previous best case, and four amplifier modules instead of six. The enhanced bunching option generates pulses with a higher peak power than the default operating mode, but the individual pulses are longer and not as well-defined, having a higher trough power and wider bandwidth. The merit function of the pulse is improved from 16.5 to 17.5, showing this is a viable alternate mode of operation for the ML-AB scheme, presenting a trade-off between higher peak power and lower output quality. Since the chicane can easily be turned on and off, this grants the scheme flexibility depending on the requirements of the user.

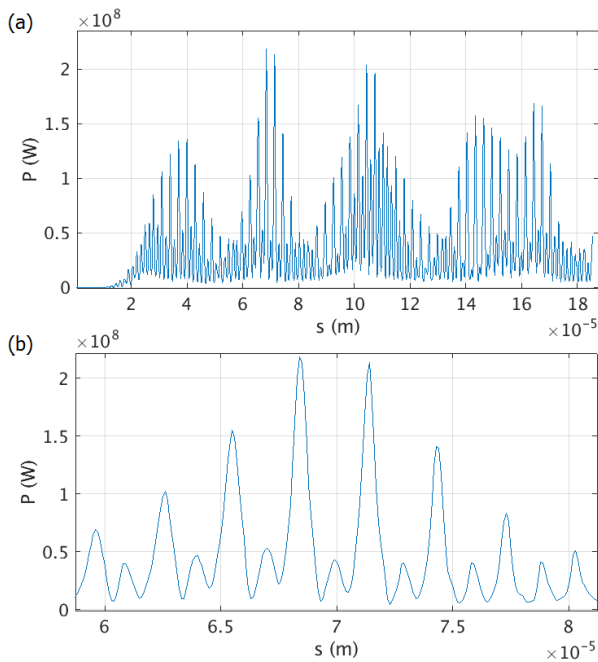


Figure 5: Enhanced bunching operation output, (a) the full pulse and (b) a detail shot of the pulse train produced.

### SPATIAL FILTERING USING APERTURE

The clean, short optical pulses created in the afterburner section are emitted along with the normal SASE radiation generated in the amplifier, which provides a level of background radiation that degrades the quality of the pulse train. Removing this SASE radiation from the output would improve the overall quality and visibility of the short pulses.

As the unwanted SASE radiation is generated in the amplifier, upstream of the afterburner where the clean pulses are produced, it has diffracted more by the end of the afterburner than the radiation generated in the afterburner. It can therefore be filtered out spatially, using a sufficiently small aperture applied during or after the afterburner section.

This was tested by applying a small circular aperture at the end of the afterburner, for the default operation mode of the scheme. The resulting power profiles at the end of the afterburner are shown in Fig. 6 with the output parameters are listed in Table 2, for an aperture of 0.2 mm. The merit function  $M$  was improved from 16.5 to 17.5. Here the aperture was placed immediately after the afterburner; a more practical but equivalent solution would be to use a larger aperture further downstream.

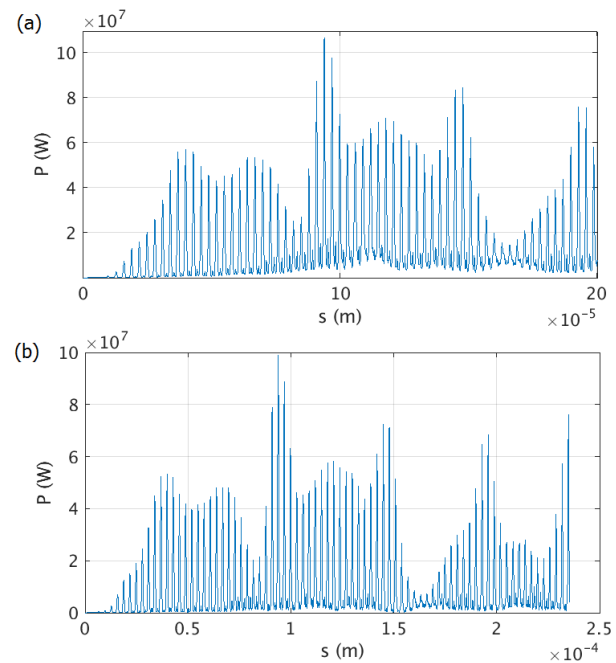


Figure 6: Output profiles after 10 afterburner modules, (a) before aperture and (b) with  $\sim 0.2$  mm aperture applied.

### CONCLUSION

The capability of the scheme to produce pulses of 126 MW peak power and approximately 2 fs duration has been demonstrated, along with an alternative operating mode that produces pulses of 219 MW peak power and 2.7 fs duration and a potential way to improve the quality of the pulses using aperture filtering. A comparison of the outputs of these schemes is seen in Table 2. The enhanced bunching and aperture filtering schemes have the same improved merit function, as although the aperture filtering produces the cleanest pulses, the enhanced bunching scheme produces pulses with nearly twice the peak power. Future work on the scheme could include investigation of harmonic generation, variable polarisation output, or use of the model to quantify relevant design tolerances.

**REFERENCES**

- [1] J. A. Clarke *et al.*, “CLARA Conceptual Design Report”, JINST 9, T05001, May 2014.
- [2] Free-Electron Laser (FEL) Strategic Review, <http://www.stfc.ac.uk/files/fel-report-2016/>
- [3] D. J. Dunning, B. W.J. McNeil, and N. R. Thompson, “Few-Cycle Pulse Generation in an X-Ray Free-Electron Laser”, *Phys. Rev. Lett.*, 110, 104801, Mar. 2013.
- [4] S. Reiche, “GENESIS 1.3: a fully 3D time-dependent FEL simulation code”, *NIMA* A 429, 243-248, Jun. 1999.
- [5] L. T. Campbell and B. W.J. McNeil, “PUFFIN: A three dimensional, unaveraged free electron laser simulation code”, *Phys. Plasmas*, 19 093119, Sep. 2012.